Correlation of excess power and helium production during D_2O and H_2O electrolysis using palladium cathodes

M.H. Miles * and R.A. Hollins

Chemistry Division, Research Department, Naval Air Warfare Center Weapons Division, China Lake, CA 93555 (USA)

B.F. Bush ** and J.J. Lagowski

Department of Chemistry, University of Texas, Austin, TX 78712 (USA)

R.E. Miles

Nuclear Safety Department, E.G.&G. Rocky Flats Inc., Rocky Flats Plant, Golden, CO 80402 (USA)

(Received 3 March 1992; in revised form 3 August 1992)

Abstract

A critical issue in determining whether or not the anomalous effects that occur during D_2O electrolysis are of nuclear origin is the measurement of nuclear products in amounts sufficient to explain the rate of excess enthalpy generation. Calorimetric evidence of excess power up to 27% was measured during the electrolysis of heavy water using palladium cathodes. Maximum excess power was 0.52 W (1.5 W/cm^3) at 250 mA/cm^2. Eight electrolysis gas samples collected during episodes of excess power production in two identical cells and analysed by mass spectrometry showed the presence of ^4He. Furthermore, the amount of helium detected correlated qualitatively with the amount of excess power and was within an order of magnitude of the theoretical estimate of helium production based upon fusion of deuterium to form ^4He. Any production of ^3He or neutrons in these experiments was below our detection limits. However, the exposure of dental X-ray films placed outside the cells suggests the emission of radiation. Control experiments performed in exactly the same way but using $H_2O + LiOH$ in place of $D_2O + LiOD$ gave no evidence of helium, excess power or radiation.

INTRODUCTION

It is now known that the observation of electrochemically induced cold fusion effects [1,2] requires special attention to many details such as cell geometry,

---

* To whom correspondence should be addressed.
** Present address: Chemistry Division, Research Department, Naval Air Warfare Center Weapons Division, China Lake, CA 93555, USA.

electrode arrangements, current density, deuterium loading and control of impurities, as well as considerable patience. Our initial efforts, representing 5 months of research, did not produce any measurable excess enthalpy effects [3]. In retrospect, it is not surprising that many research groups were unsuccessful in their few weeks of frenetic cold fusion activities [4,5]. The low intensity of neutrons has prompted proposals of nuclear processes that yield only heat and helium as products [6–10]. We report here the results of electrochemical calorimetric experiments designed to detect helium in the effluent gases while rigorously excluding possible helium contamination from other sources. Evidence for the occurrence of nuclear events was obtained by the measurements of ^{4}He, excess power and radiation during the electrolysis of the $Pd/D_2O + LiOD$ cells. There was no experimental evidence for nuclear events in the $Pd/H_2O + LiOH$ control systems.

EXPERIMENTAL

The electrolysis cell initially contained 18 g of 0.2 M $LiOD + D_2O$ (99.9%, Cambridge Isotope Laboratories). The palladium rod cathode (Johnson Matthey, 99.96%, $d = 0.63$ cm, $l = 1.1$ cm) was spot-welded to a nickel lead. A helically wound coil of $Pt + 20\%$ Rh (5.35 g, $d = 0.1$ cm) with about four windings per centimeter of cathode length served as the counter-electrode and was symmetrically positioned about 0.3 cm from the outer surface of the cathode. This configuration establishes a uniform potential over the surface of the cathode that is favorable for charging [2]. Both the anode and cathode leads were covered with heat-shrinkable Teflon tubing to prevent exposure of the bare metal to the gases in the headspace. Two identical isoperabolic calorimetric cells were always run in series (cells A and B) in a constant-temperature bath set at 27.50°C. The calorimetric cell design consisted of a glass test tube ($l = 15$ cm, $d = 1.8$ cm) containing the anode, cathode and electrolyte that was placed in a larger glass tube potted in an insulated jacket. The larger glass tube contained a constant volume of H_2O that served as a heat transfer medium and acted as an integrator for the heat output of the electrolysis cell. The electrolysis cell in this configuration can be visualized as a resistive heater element with the temperature being measured in the secondary compartment. This cell design minimized the decrease in the calorimetric cell constant that occurs during electrolysis because of the decrease in the electrolyte volume [2,3]. Furthermore, this design of a long thin electrolysis cell of small volume and one short dimension allows the excess enthalpies to become large compared with experimental errors [2]. Further details of the calorimetric cell design and determinations of the calorimetric constants K_i are given elsewhere [11]. Previously determined mean values of these constants [11] were used in this study ($K_1 = 0.138$ W/°C, $K_2 = 0.143$ W/°C and $K_4 = K_5 = 0.135$ W/°C for the four thermistors in cells A and B). The constants were determined in four separate experiments over a 1 year period and showed standard deviations of less than $\pm 3\%$ with no significant change with time. Calibrations were also determined by Joule heating using a 20 Ω resistor as described previously [11]. The time constants

for our calorimeters were determined to be about 30 min; thus any change in cell conditions, such as D_2O additions, yielded accurate calorimetric measurements after a 3 h time period.

Measurements correlating the time of excess power production and the generation of helium in the electrolysis gas stream require the use of open calorimetric systems. Rigorous efforts were made to avoid contamination of the electrolysis gas from atmospheric helium. The system was always under positive pressure since the effluent gas was evolved through an oil bubbler. Details of the gas collection system are given elsewhere [12]. The entire system was thoroughly flushed with boil-off nitrogen that contained no detectable helium [12]. Furthermore, the system was self-flushing owing to the steady evolution of D_2 and O_2 gases. The gas evolution rate was calculated to be 6.73 ml/min at 528 mA (200 mA/cm^2) at 297 K and 700 Torr assuming ideal gas behavior. Actual measurements of the gas evolution rate by the displacement of water yielded 6.75 ± 0.25 ml/min for cell A and 6.69 ± 0.15 ml/min for cell B. These data add to the substantial evidence that excess enthalpy effects cannot be explained by the recombination of D_2 and O_2 gases within the cell [11,13–16].

Eight round-bottom flasks (500 ml, Pyrex) were converted to Schlenk flasks by the addition of a glass stopcock, followed by flame and oven annealing, and vacuum leak testing prior to use. These flasks were also routinely soaked in a base bath (KOH + EtOH). All glass joints were carefully lapped for a concentric fit and lubricated with silicon grease (Dow Corning, High Vacuum). These flasks, used for the collection and shipment of effluent gas samples, were cross-taped (filament tape) to reduce fragmentation danger in case of any explosions. The average glass wall thickness determined volumetrically for a typical flask using $4\pi[(r + d)^3 - r^3]/3$ was $d = 1.8$ mm.

The electrolysis gas samples collected at China Lake in the 500 ml flasks were sent to the University of Texas for analysis by mass spectrometry; details of these measurements are reported elsewhere [12]. A cryofiltration system was employed to remove all gases except helium. Mass spectral measurements had sufficient resolution to baseline to separate D_2 and ^{4}He. Based on air samples collected in the Chemistry Laboratory at the University of Texas and assuming a normal helium concentration of 5.22 ppm by volume [17], the detection limit for helium in our measurements (signal-to-noise ratio 2:1) is approximately 8×10^{11} atoms of ^{4}He in 500 ml of the nitrogen gas reference [12]. Because of the use of helium-cooled nuclear magnetic resonance instruments and helium-filled glove-boxes in the building, the helium content of the laboratory air can be significantly higher than 5.22 ppm and was recently measured as 10.27 ± 0.03 ppm and 9.89 ± 0.03 ppm in two separate experiments. These results suggest a detection limit of about 2×10^{12} atoms of ^{4}He in 500 ml of nitrogen or about 0.1 ppb. Higher detection limits are to be expected for $D_2 + O_2$ electrolysis gas samples because of different adsorption properties in the cryofilter. A commercial laboratory (Helium Field Operations, Amarillo, Texas) used in later experiments reported a detection limit of 1–2 ppb for helium in $D_2 + O_2$ electrolysis gas samples.

Indium ($d = 0.25$ mm, 2.2 g) and gold ($d = 0.5$ mm, 14 g) foils mounted at the surface of the electrochemical cells were used in attempts to detect any sustained neutron emission rates of 10^4 neutrons/s or higher [18]. A neutron survey meter (Ludlum model 15) was always kept close to the water bath containing the two electrochemical cells. A Geiger–Mueller (GM) α-β-γ detector with a thin end window (Ludlum model 44-7) was positioned about 20 cm from the tops of the electrochemical cells and connected to a scaler ratemeter (Ludlum model 2200) and a printer (Casio HR-8A). Dental X-ray film (Kodak Ultra-speed, DF-58) placed near the outside surface of the electrochemical cells was also used to detect any radiation.

RESULTS

The calibration of calorimetric cell A filled with D_2O by Joule heating with a 20 Ω resistor is shown in Fig. 1. The results are linear over the power range used (0–3.04 W) with correlation coefficients better than 0.999 ($n = 10$). The two distinct lines are a result of differences in the two thermistors (T_1, T_2) rather than any temperature gradients within the cell (T_1 is positioned higher). Similar Joule heating calibrations for cell B (0–3.53 W), presented in Fig. 2, give almost the same temperatures for these thermistors (T_4 and T_5, with T_4 positioned higher); hence only the line through the mean temperature values is shown. Thermistors T_4 and T_5 are very closely matched as reflected by their identical calorimetric cell constants ($K_4 = K_5$). Figure 2 combines calibrations with both D_2O- and H_2O-filled cells performed before and after our heat and helium studies, yet no significant
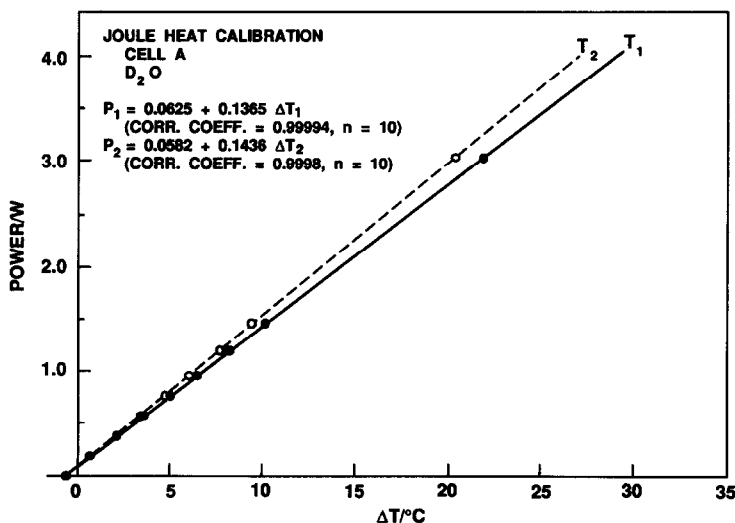

Fig. 1. Calibration of calorimetric cell A filled with D_2O using Joule heating (20 Ω resistor).
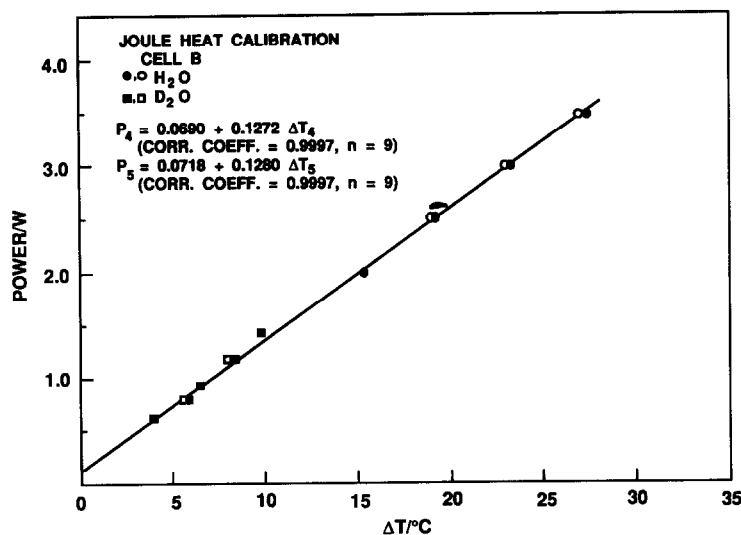
Fig. 2. Calibration of calorimetric cell B filled with H_2O (●, ○) or D_2O (■, □) using Joule heating (20 Ω resistor).

difference is observed. The linear results (Figs. 1 and 2) are in agreement with Newton's law of cooling and show that excellent heat recovery can be obtained with our calorimetric cell design. Although there is no electrolysis power and hence no gas evolution during these calibrations by resistor power, the relationship $P = K \Delta T$ for a typical electrolysis power of 2.00 W yields K values ranging within 98.5% (K_5) to 103.5% (K_2) of the constants used in this study.

Calorimetric studies using palladium rod cathodes in 0.2 M LiOD + D_2O are presented in Fig. 3. The equation

$$X = \frac{\text{power out}}{\text{electrolysis power}} = \frac{K \Delta T}{(E - E_H^\circ)I} \tag{1}$$

was used, where K is the calorimetric cell constant, E is the cell voltage, E_H° is the thermoneutral potential and ΔT is the temperature difference [11]. Because of the time constant of the calorimeter (30 min), a time-averaged effect of any excess power is always observed experimentally; hence the use of the term excess enthalpy can also be justified. Excess power (enthalpy) is present when $X > 1.00$, where X is the daily mean value of the power ratio. Gas sample collection dates for helium analysis are given for cells A and B; thus the highest excess power (27%) was observed on 21 October 1990 in cell B. This value may actually be somewhat higher since the weekend room temperature (21.5°C) was cooler than normal (23°C). The first 12 days are not shown in Fig. 3 because the electrolysis was shut down several times to correct leaks in the gas-collection system. No significant excess enthalpy effects were observed in the first 10 days.
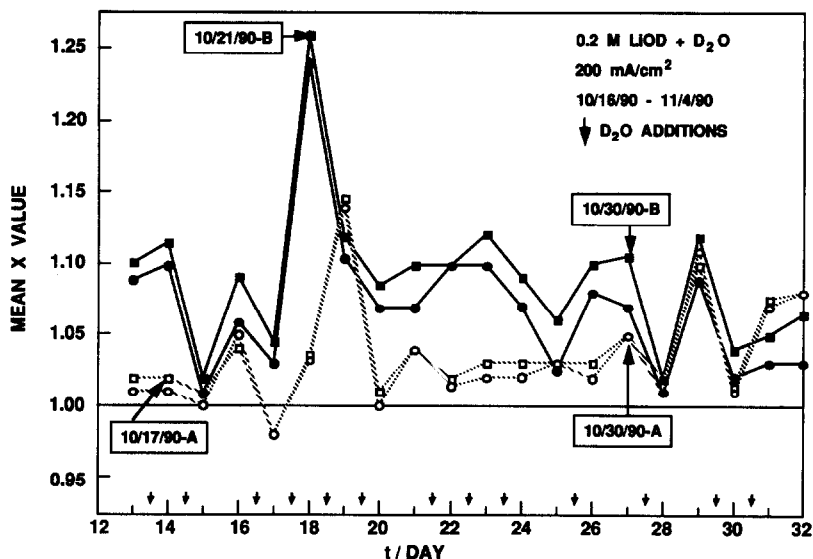
Fig. 3. Calorimetric measurements and effluent gas collection dates in $D_2O + LiOD$ for cell A (○, □) and cell B (●, ■).

The continuation of the calorimetric measurements and the collection of effluent gases for helium analysis are shown in Figs. 4–6. Indium foils were placed around the outer wall of both electrolysis cells at the end of day 33 (Fig. 4). The current was accidentally interrupted during this process, and neither cell showed significant excess enthalpy the following day. The indium foils were replaced by gold foils at the end of day 64 in cell A and day 70 in cell B (Fig. 5). The current density was increased to 250 mA/cm^2 at the end of day 66 (Fig. 5). The gold foils were removed and replaced by dental films at the end of day 76 (Fig. 6). The current was again accidentally interrupted for a few minutes during this procedure, but only cell A showed a loss of the excess enthalpy effect the following day. The cells were turned off and the dental films removed on 25 December 1990 (Fig. 6). Calorimetric results around 17 December 1990 are questionable for cell B because of the unusual increases in the cell voltage with time as the D_2O solution level dropped below the electrode level. This problem was not fully understood and corrected until the dental film was inserted on 18 December 1990 (Fig. 6).

The helium analysis results in Table 1 show that the effluent gases contained ^4He when the electrolysis of D_2O produced significant excess power. No ^3He was detected. Small peaks near the detection limit of the mass spectrometer (signal-to-noise ratio 2:1) are assigned a value of 10^{12} atoms of ^4He per 500 ml of effluent gases based on a detection limit of 0.1 ppb. Actual values would be higher since the adsorption of the $D_2 + O_2$ electrolysis gas sample in the cryofilter is slower than the adsorption of the N_2 reference gas. Medium peaks were roughly an order of magnitude greater while large peaks were about two orders of magnitude above
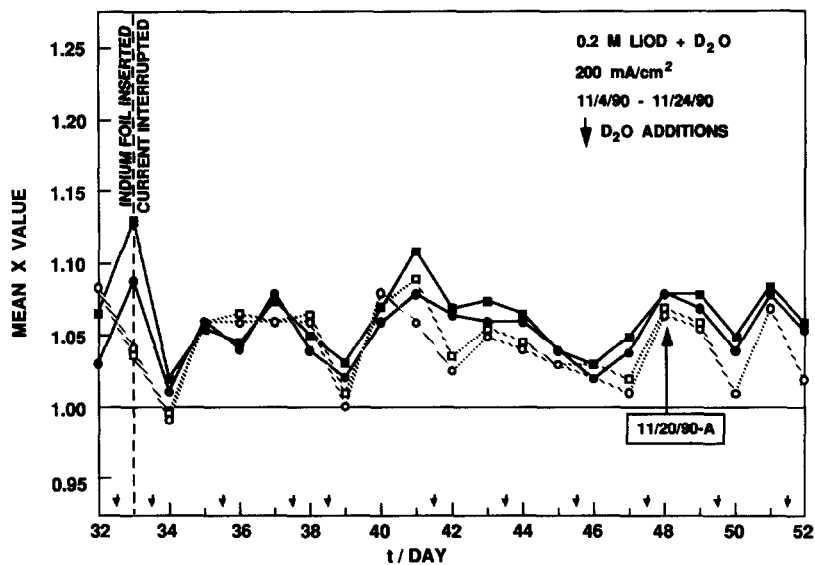
Fig. 4. Continuation of calorimetric measurements and effluent gas collections in $D_2O + LiOD$ for cells A and B. Indium foil activation experiments began on day 33.
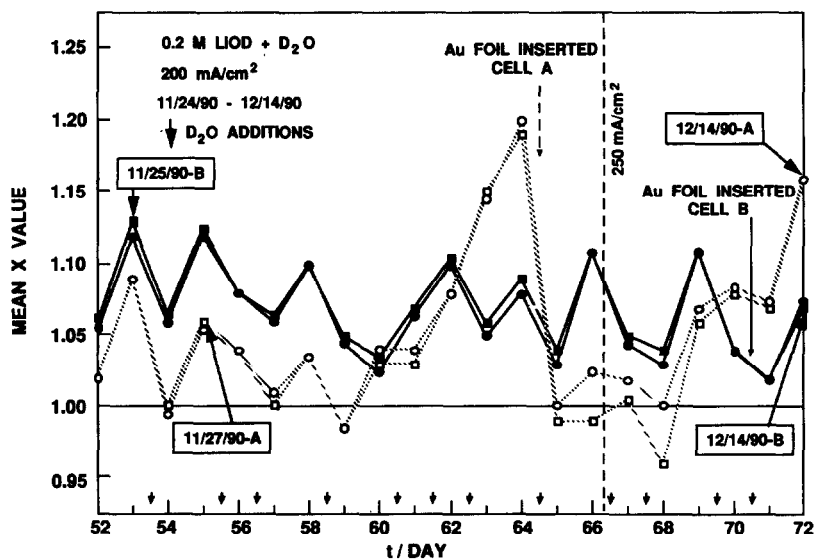

Fig. 5. Continuation of calorimetric measurements and effluent gas collections in $D_2O + LiOD$ for cells A and B. Gold foil activation experiments began on day 64 for cell A and on day 70 for cell B.
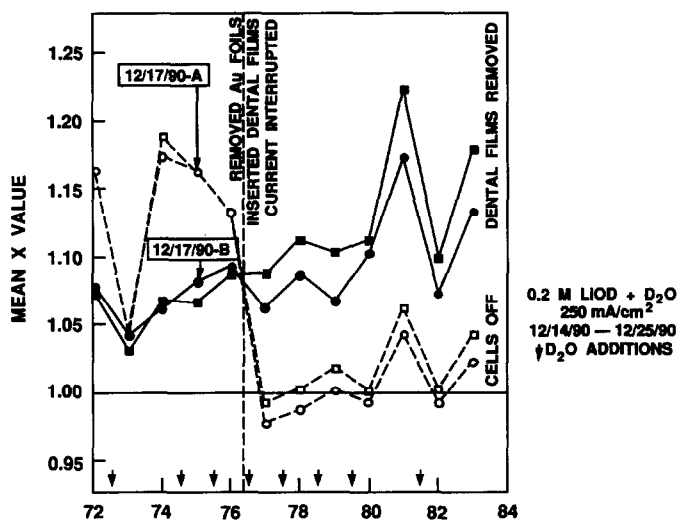
Fig. 6. Final portion of calorimetric measurements and effluent gas collections in $D_2O + LiOD$ for cells A and B. Dental film experiments began on day 76.

the detection limit. The values reported for the excess power P_{EX} and power ratios X in Table 1 are those measured within 1–2 h of removing the gas collection flask in order to obtain the best time correlation. The excess power measurements were always quite steady during this time period. The samples are arranged in order of decreasing power except for the 12/17/90-B sample where the low D_2O level is likely to have created a calorimetric error. The only sample not listed in Table 1 is 12/14/90-B because the flask broke during shipment. The input power for each

TABLE 1

Helium production during D_2O electrolysis

Sample	P_{EX}	X	^{4}He atoms/500 ml [a]
12/14/90-A	0.52 [b]	1.20 [b]	10^{14} (large peak)
10/21/90-B	0.46	1.27	10^{14} (large peak)
12/17/90-A	0.40 [b]	1.19 [b]	10^{13} (medium peak)
11/25/90-B	0.36	1.15	10^{14} (large peak)
11/20/90-A	0.24	1.10	10^{13} (medium peak)
11/27/90-A	0.22	1.09	10^{14} (large peak)
10/30/90-B	0.17	1.12	10^{12} (small peak)
10/30/90-A	0.14	1.08	10^{12} (small peak)
10/17/90-A	0.07	1.03	$< 10^{12}$ (no peak)
12/17/90-B	0.29 [b,c]	1.11 [b,c]	$< 10^{12}$ (no peak)

[a] No ^{3}He was detected; mass spectrometer always at highest sensitivity.
[b] $j = 250$ mA/cm^2; all other experiments used $j = 200$ mA/cm^2.
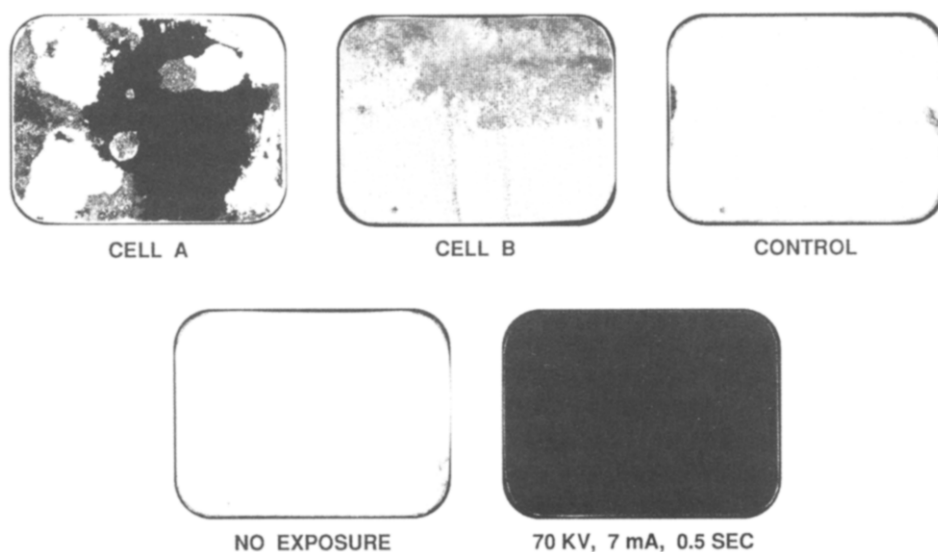[c] Possible calorimetric errors due to low D_2O solution levels.

Fig. 7. Results of dental film experiments in cells A and B as well as in a control study. Samples of fresh films with no exposure and total exposure are also shown for comparison.

measurement is given by $P_{EX}/(X - 1.00)$; hence the input power is 2.60 W for the 12/14/90-A sample. It should be mentioned that the results of excess power measurements were generally not released until the helium analysis was completed.

Results of dental film experiments are shown in Fig. 7. The film wrapped around the outside of the electrolysis cell A was the closest to the palladium and showed the greatest exposure. Clear regions are due to a peeling away of the emulsion rather than non-exposure due to some water seepage into this film. These films were positioned within the distilled water contained in the secondary (gap) compartment [11]. The film in cell B was further away from the palladium and deeper in the secondary compartment; hence the bottom half was somewhat shielded by the Teflon pedestal used to hold the palladium in position [11]. This film showed partial exposure with even less exposure near the bottom portion where any direct radiation would have to pass through the Teflon pedestal. The control film was immersed in distilled water for the same time period and showed only scattered exposure attributed to background radiation. Samples of fresh films with no exposure and total exposure are also shown for comparisons. As shown in Fig. 6, cell A was producing the larger excess power effect when the film was first inserted, but cell B produced the larger effect in the 7 days that followed.

Control experiments are of major importance in proving helium production in cold fusion experiments. These control studies involved the use of H_2O + LiOH in place of D_2O + LiOD, yet the same cells, electrodes, gas lines and collection flasks were employed exactly as with D_2O. Results of the H_2O control experiments are

TABLE 2

Results of $H_2O + LiOH$ control experiments

Sample [a]	Results [b]
1/16/91-A	No ^{4}He or ^{3}He observed
1/16/91-AA	No ^{4}He or ^{3}He observed
1/16/91-B	No ^{4}He or ^{3}He observed
1/17/91-A	No ^{4}He or ^{3}He observed
1/17/91-B	No ^{4}He or ^{3}He observed

[a] Used same cells, electrodes, gas lines, and collection flasks as in D_2O experiments; $j = 200$ mA/cm^2.
[b] Mass spectrometer always at highest sensitivity; any gas passing through the cryofilter was allowed time to accumulate and then surged into the mass spectrometer.

shown in Table 2. No helium was observed in any experiment. The $H_2O + LiOH$ electrolysis, conducted in an identical manner to the $D_2O + LiOD$ electrolysis, is the best indication of our ability to exclude ^{4}He contamination from the air. The $H_2O + LiOH$ experiments did not produce any significant excess power or exposure of dental film. The mean calorimetric values for 15 days of electrolysis are $\bar{X}_1 = 1.025 \pm 0.02$, $\bar{X}_2 = 1.035 \pm 0.03$ for cell A and $\bar{X}_4 = 1.01 \pm 0.02$, $\bar{X}_5 = 1.00 \pm 0.03$ for cell B at the 99% confidence interval (± 2.58 $\sigma/\sqrt{n}$, $n = 15$). Earlier reports of unexplained excess heat effects in $H_2O + LiOH$ [12] were due to errors related to the dental film studies. The secondary compartments containing the films were not tightly sealed; hence loss of water by evaporation or possibly by a wicking action created a calorimetric error. We reported previously that there is a 2% increase in X per milliliter of H_2O lost from the gap [11].

Previous calculations suggest that neutron activation of indium or gold foils should occur for emission rates greater than 10^4 s^{-1} if the foils are placed at the outer glass surface of our electrochemical cell [18]. No activation of indium or gold foils was detected in this study; hence the average emission rates were less than 10^5 s^{-1} during the time period that these foils were in the cells. The establishment of a lower detection limit would have been possible for gold foils using a multichannel analyzer; however, the foils used in our experiments were unfortunately lost for about a week despite express shipment to E.G. & G. Rocky Flats Inc., Golden, CO, for activation analysis. There were generally no responses significantly above the background levels for the neutron survey meter, but the GM detector gave several periods of unexplained high count rates. Any γ-ray production would deposit little heat in the cell since most of the energy would be carried off by the photon [19]. Recent experiments with the GM detector placed much closer (5 cm) to the $Pd/D_2O + LiOD$ cells have shown sporadic periods of elevated counts that are apparently triggered by changes in the electrolysis conditions.

Tritium measurements on the final $D_2O + LiOD$ solutions gave 410 dpm/ml (disintegrations per minute per milliliter) for cell A and 375 dpm/ml for cell B compared with 230 dpm/ml for the $D_2O + LiOD$ sample that was never subjected

to electrolysis. Although this 78% increase in tritium content for cell A is considerably larger than the 19% increase observed in previous experiments [11], it is still not possible to rule out electrolytic enrichment or variations in the tritium content of the D_2O used as possible explanations [20].

Subsequent experiments using new palladium electrodes in $D_2O + LiOD$ (0.2 M) failed to produce any excess enthalpy, dental film exposure or high count rate periods with the GM detector. The mean calorimetric values were $\overline{X}_1 = 0.97 \pm 0.02$, $\overline{X}_2 = 1.02 \pm 0.01$ for cell A and $\overline{X}_4 = 1.00 \pm 0.02$, $\overline{X}_5 = 0.98 \pm 0.01$ for cell B at the 99% confidence interval ($n = 35$). The continuation of this study for another 40 days (April–May 1991) gave similar results. This experiment illustrates the reproducibility problem in cold fusion investigations [21–26]. In addition to the use of new palladium electrodes, other experimental changes included sealing the bottom of the palladium rods with epoxy, less symmetrical electrode arrangements, less exposure of $D_2O + LiOD$ to atmospheric CO_2 and the use of D_2O from a different lot number. The significance, if any, of these factors is not known. Recent analysis of the D_2O used suggests that water contamination was not a significant problem.

DISCUSSION

The amount of helium (^{4}He) observed in the gaseous products maintained a qualitative correspondence to the amount of excess power observed in electrochemical calorimetric cells (Table 1). This indicates that ^{4}He is produced at or near the surface of the palladium electrode rather than deeper in the bulk metal and that most of the helium escapes from the electrode and resides in the electrolysis gas. Several theories have predicted this behavior [9,10]. A previous study of helium in electrolyzed palladium rods supplied by Fleischmann and Pons also supports a surface-related mechanism [27].

Although the exact nature of the reaction(s) producing the excess power effect is not known, the fusion process

$$^2D + {}^2D \rightarrow {}^4He + 23.8 \text{ MeV (lattice)} \tag{2}$$

can be used as a basis for an estimate of helium production. For this reaction 1 W corresponds to a rate of 2.62×10^{11} ^{4}He/s. The highest excess power observed at 528 mA (0.46 W, 10/21/90-B, Table 1) would therefore produce 5.4×10^{14} atoms of ^{4}He in the time period required to fill the 500 ml collection flask with D_2 and O_2 gases (4440 s). About 10^{14} atoms of ^{4}He were detected, which is within experimental error of the theoretical amount. Difficulties in detecting nuclear products in electrochemical fusion experiments stem from the fact that fusion reactions are a million times more energetic than ordinary chemical reactions [28]. For example, when operating at 1 W of excess power, the reaction described by eqn. (2) would require 73 000 years to produce a single mole of helium (4.0 g). The excess power is much more readily detected than the helium product [26].
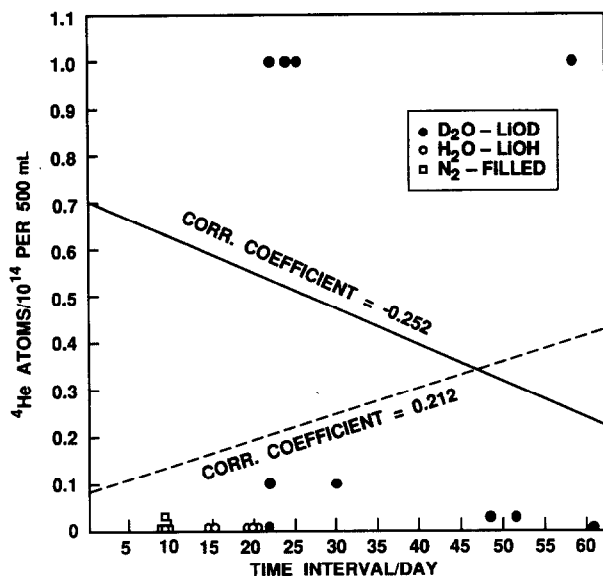
Fig. 8. Amount of helium observed versus the storage time interval between gas collection and helium analysis. These experimental results show no measurable effect of atmospheric helium diffusing into the Pyrex glass flasks containing D_2 or H_2.

Despite the qualitative correlation of excess power and helium, we are concerned with possible sources of error which include air contamination, helium diffusion into the glass flask and the escape of helium contained in the palladium rod. Ignoring the helium–heat relationship (Table 1), the simple yes or no detection of helium in eight out of eight experiments producing excess heat and the absence of helium in six out of six experiments not producing excess heat (one in D_2O, five in H_2O) implies a chance probability of only $(1/2)^{14} = 1/16384$ or 0.0061%. Therefore atmospheric contamination does not provide a likely explanation for our ^4He measurements.

The diffusion of helium through glass, which is a valid concern, can be expressed by

$$q = KP/d \tag{3}$$

where q is the permeation velocity, K is the permeability, P is the partial pressure of helium and d is the glass thickness [29,30]. The value of K varies greatly with the type of glass, its treatment and temperature [29,30]. For the Pyrex glass flasks used in this study ($d = 1.8$ mm), theoretical calculations yield $q = 8.3 \times 10^9$ He/cm^2/day or 2.6×10^{12} He/day ($A = 314$ cm^2). Experimentally, however, we find no measurable evidence for any effect due to helium diffusion through glass. The amount of helium observed versus the time interval that the effluent gas sample resided in the glass is shown in Fig. 8. For $D_2O + LiOD$ experiments, high and low helium levels occur at both short and long time intervals that ranged from

TABLE 3

Experimental helium diffusion rates in nitrogen-filled 500 ml flasks (Pyrex, $A = 314$ cm^2, $d = 1.8$ mm)

Time/days	Measured ^{4}He/atoms	Diffusion rate/atoms per day
14 [a]	47×10^{12}	3.4×10^{12}
44.6 [b]	167×10^{12}	3.7×10^{12}
65 [a]	170×10^{12}	2.6×10^{12}

[a] Helium Field Operations, Amarillo, TX.
[b] Rockwell International, Canoga Park, CA.

22–61 days. In fact, linear regression shows a negative correlation if any exists at all. For H$_2$O + LiOH experiments, no helium was detected for gas resident periods of up to 20 days. However, some helium was detected in nitrogen-filled flasks and was attributed to possible flask leakage [12].

A possible explanation for the lack of measurable helium diffusing through the glass is the opposing flow of deuterium or hydrogen out of the glass. Since deuterium makes up two-thirds of the gas within the flask, its rate of diffusion outward is about three orders of magnitude greater than the diffusion of atmospheric helium into the flask. Helium and hydrogen (deuterium) diffuse through glass by similar mechanisms using the same "lattice" sites [29,30] and show similar kinetic parameters [31]. Furthermore, hydrogen removes helium from glass [32]. Although no specific literature study of the effect of hydrogen on the diffusion of helium through glass could be found, Paneth and Peters [33] have reported that after 15 days fewer than 3×10^9 He atoms had diffused into a 3 l flask ($A = 1300$ cm^2) containing 10 Torr of hydrogen gas. Preliminary results from two different laboratories indicate that the rate of atmospheric helium diffusion into our flasks is two to three times slower for flasks containing hydrogen or deuterium rather than nitrogen.

Table 3 presents results from two different laboratories relating to helium diffusion into our flasks when they were filled with nitrogen. Our previous report of possible flask leakage [12] could be explained by helium diffusion into nitrogen-filled flasks. Saturation of the glass with deuterium or hydrogen in prior experiments could affect the helium diffusion rates. Measurements by the two laboratories were performed several months after our helium measurements were completed, hence any effects due to deuterium or hydrogen saturation of the glass would probably have dissipated. The best evidence against any significant helium diffusion through glass in our experiments is our H$_2$O + LiOH control studies (Table 2) and the absence of any time correlation (Fig. 8) for our helium measurements.

Samples of our unused palladium were analyzed for helium by Rockwell International. No ^{3}He or ^{4}He was observed in any of our palladium samples. In terms of helium concentrations, the uncertainties correspond to less than 10^8 atoms/mg for ^{3}He and ^{4}He. This indicates that our palladium cathodes originally contained fewer than 5×10^{11} He atoms; hence any helium originally present in

the palladium electrode is not sufficient to explain our measurements. Furthermore, the same palladium electrodes had been used in four previous experiments [11]. A sample of the palladium electrode used in these $D_2O + LiOD$ and $H_2O + LiOH$ experiments also failed to show any significant level of ^3He or ^4He. This result is somewhat inconclusive, however, since the palladium electrodes were polished after the D_2O study that produced excess heat and helium and were then used in the $H_2O + LiOH$ study (Table 2). Previous studies of electrolyzed palladium rods supplied by Fleischmann and Pons also showed no ^3He above the detection limit; hence conventional D–D fusion reactions were judged unlikely as the source of excess heat [27]. Measurements of ^4He within the palladium were inconclusive in confirming the existence or nonexistence of electrolytically induced fusion via helium production [27]. Liaw and coworkers [34,35] have reported the enhancement of ^4He in palladium samples from an electrode that produced at least 600% excess power.

Another experiment indicating a correlation of excess power and helium used a modification of the Szpak codeposition method [36]. Palladium ions were generated electrochemically in the 0.3 M LiCl electrolyte by reversing the current followed by normal cell operation which resulted in the simultaneous deposition of palladium and deuterium to produce the excess enthalpy effect. Effluent gas samples sent to a commercial laboratory (Amarillo, Texas) (Table 3) yielded 7.0 ± 2 ppb ^4He or 8.5×10^{13} $^4He/500$ ml for a cell producing 0.14 W of excess power $(X = 1.12)$ at 528 mA. This sample was within a factor of 2 of the theoretical amount of ^4He based on eqn. (2). A second gas sample gave 7.5 ± 2 ppb ^4He or 9.2×10^{13} $^4He/500$ ml for a cell producing 0.54 W of excess power $(X = 1.25)$ at 874 mA. Some recombination of D_2 and O_2 was observed in this cell; hence the measured excess power is too high. Although the amount of detected helium was higher than in a nitrogen-filled flask (Table 3), no other controls were included in these measurements. Further work relating to helium measurements has been hindered by difficulties in obtaining the excess power effect.

The addition of D_2O at intervals of 1–3 days is often followed by a decrease in the mean X value (Figs. 3–6). The D_2O additions decrease the electrolyte concentration, and hence a significant increase in the cell voltage E occurs. Even if the excess enthalpy effect remains constant, a decrease in X will occur due to the increase in E. For example, eqn. (1) can be rewritten as

$$X = \frac{K(\Delta T_{EL} + \Delta T_F)}{(E - E_H^\circ)I} = 1 + \frac{K \Delta T_F}{(E - E_H^\circ)I} \tag{4}$$

where ΔT_{EL} is the net temperature change due to the electrolysis power and ΔT_F is the net change in temperature produced by fusion. When excess heat is present $(X > 1.00, \Delta T_F > 0)$, an increase in E will produce a decrease in X if ΔT_F remains constant. A decline in X was observed following 30 out of 44 D_2O additions (Figs. 3–6) for both cell A and cell B. An increase in X following the D_2O addition would require a significant increase in fusion rate to boost ΔT_F. The addition of D_2O produces a sudden reduction of the cell temperature followed by

a gradual rise to a higher temperature as well as solubility changes for surface species and possible changes in the bubble pattern of the evolving gases; thus fusion processes at the electrode surface would probably be affected. The most pronounced upward thermal ramp occurred following D_2O addition (Fig. 3, day 18). Lewis and Sköld [37] have also noted upward thermal ramps following D_2O addition.

The major errors in our calorimetric measurements are probably fluctuations in the room temperature and fluctuations in the cell voltage due to gas bubble effects. These error sources limit our accuracy to about ± 0.04 W or $\pm 2\%$. Nevertheless, the major error source in correlating the amount of helium with the excess enthalpy is in the helium analysis. Improved measurements of helium and excess enthalpy could identify precisely the energy of the dominant fusion reaction.

The effect of room temperature stems from the exposure of the top of our calorimetric cell to the atmosphere. Hence

$$P = Q_b + Q_t \tag{5}$$

where Q_b and Q_t are the rates of heat flow out into the bath and out of the top respectively. Therefore

$$P = K_b(T_2 - T_b) + K_t(T_2 - T_R) \tag{6}$$

where K_b and K_t represent fractions of the calorimetric constant for heat flow into the bath and out of the top respectively, T_2 is the cell temperature, T_b is the bath temperature and T_R is the room temperature. Rearranging eqn. (6) gives

$$P = (K_b + K_t)T_2 - K_bT_b - K_tT_R \tag{7}$$

Hence

$$\left(\frac{\delta P}{\delta T_2} \right)_{T_b, T_R} = K_b + K_t = K \tag{8}$$

and

$$P = K \, \Delta T + K_t(T_b - T_R) \tag{9}$$

where $\Delta T = T_2 - T_b$. Equations (8) and (9) show that a linear relationship is expected for all power levels as long as T_b and T_R remain constant. Furthermore, the loss of heat out of the top yields a positive intercept for $\Delta T = 0$ as shown in Figs. 1 and 2. Intercept values yield $K_b = 0.12$ W/K and $K_t = 0.02$ W/K for our calorimeters; hence about one-seventh of the heat flow is out of the top of the cell. Furthermore, a change in room temperature of only 2°C produces an error of 0.04 W or a 2% error for a typical power input of 2 W. This error source can be reduced by placing the bath in a carefully thermostated atmosphere or by adding insulating material to the cell top. The bath level itself can also be a source of error. In our experiments, lowering the bath level by about 2 cm produced a 3% increase in the apparent excess heat. The convection heat transfer coefficient for air is 20–40 times smaller than that for water [38]; thus this large difference more

than compensates for the bath temperature (27.50°C) being higher than the air temperature.

The effect of the dropping electrolyte level [39] was examined in a previous study [3] and minimized by our cell design [3,11]. Nevertheless, excessive loss of electrolyte resulting in exposure of the electrodes can produce calorimetric errors and even possible recombination of the electrolysis gases on the exposed Pt and Pd surfaces. Effects due to evaporation of D_2O and formation of PdD_n [40,41] can be expressed as

$$P_{out} = K\ \Delta T + P_{evap} + P_{charg} \tag{10}$$

Our rate of D_2O loss by evaporation (0.19 cm^3/day) yields $P_{evap} = 0.0054$ W. Using a mean value of $\Delta H_{f,PdDn} = -35\,100$ J/mol D_2[40] and assuming that the formation of PdD_n is complete within 8 h yields an average value of $P_{charg} = -0.025 \times n$ to obtain power in watts. Compared with typical $K\ \Delta T$ of 2 W, these error sources are small and tend to cancel. The effect of the formation of PdD_n would also diminish with time as the electrode becomes fully charged.

Although the experiments by Lewis and coworkers [42,43] are often cited as evidence against electrolytically induced fusion [5], the reported increase in heating coefficients (h.c.) from 14.0 to 15.9°C/W [42] suggests an excess power effect of over 13% in D_2O + LiOD. The heating coefficient can be expressed similarly to eqns. (4) and (8) as

$$\text{h.c.} = K^{-1} = \left(\frac{\delta T_2}{\delta P}\right)_{T_b,T_R} = \frac{\Delta T}{P_T} = \frac{\Delta T_{EL} + \Delta T_{Re} + \Delta T_F}{P_{EL} + P_{Re} + P_F} \tag{11}$$

where ΔT_{EL}, ΔT_{Re} and ΔT_F represent the net cell temperature changes due to the electrolysis power P_{EL}, the resistor power P_{Re} and any fusion power P_F respectively. Although ΔT is readily measured experimentally, the total output power P_T required for calibration purposes cannot be determined when an unknown amount of P_F is present. In H_2O electrolysis or the early stages of D_2O electrolysis, where $P_F = 0$, the true heating coefficient can be evaluated using eqn. (11). However, when excess power is present, ΔT includes a contribution from P_F, i.e. ΔT_F; thus a larger heating coefficient is calculated if it is simply assumed that $P_T = P_{EL} + P_{Re}$ as in the study by Lewis et al. [42]. This error is obviously due to the neglect of the unknown amount of P_F in determining the total power. According to Newton's law of cooling [38], the temperature difference ΔT defines the total output power from the cell to its surroundings. The sum $P_{EL} + P_{Re}$ can only define the input power to the electrolysis cell. Recalibrations using the load-resistor method of Lewis and coworkers [42,43] would simply zero out the unknown amount of anomalous power by increasing the heating coefficient. The assumption of a heating coefficient of 14.0°C/W in the experiment by Lewis et al. [42] yields an excess power of 1.0 W/cm^3 Pd at 140 mA/cm^2 after 161 h of electrolysis. This excess power density is in excellent agreement with our experiments (1.3 W/cm^3 Pd at 200 mA/cm^2) as well as the results reported by Fleischmann et al. [2].

The calibration of calorimetric electrolysis cells must be performed either when no excess power is present or by methods that include the excess power term in the equations and allow for its evaluation. In solving the differential equation governing the behavior of their open calorimeter, Fleischmann et al. [2] assume that the excess power is constant throughout any given measurement cycle. If P_F is constant, then eqn. (11) can be expressed as

$$K^{-1} = \left[\frac{\delta(\Delta T_{EL} + \Delta T_{Re})}{\delta(P_{EL} + P_{Re})} \right]_{T_b, T_R, P_F} \tag{12}$$

The condition of constant P_F for cell calibrations would most probably be achieved by keeping the electrolysis power constant and varying only the resistor power since the excess power increases with the current density [2,22]. In the studies by Lewis et al. [42], it is interesting to note that the sum $P_{EL} + P_{Re}$ required to maintain a constant cell temperature in 0.1 M LiOD + D_2O is always greater for the experiment at the lower current density. Although this effect is small, it is consistent with the presence of an anomalous power that increases with the current density and is near the magnitude reported by Fleischmann et al. [2].

We have found no experimental evidence of any significant changes in our calorimetric cell constants over many different experiments. The same cell constants are obtained in both D_2O and H_2O (see Fig. 2). However, for calorimetric designs where the cell temperature is measured directly in the electrolyte, the calorimetric cell constants will vary with the electrolyte level [2,3,19,39,44]. Although not discussed in their reports, this electrolyte level effect may also contribute to the rather large variations in the heating coefficients in the calorimetric experiments performed by Lewis and coworkers [42,43]. A consequence of continuous electrolysis is that any calibration is only valid for a particular liquid level [44]. Perhaps all electrochemical calorimetric results relating to cold fusion should be independently reviewed with respect to their calibration procedures, treatments of the electrolyte level effect and accuracy in determining any excess power.

Accurate calorimetric results can be obtained with either open or closed electrolysis systems if properly designed experiments and correct calibration procedures are used. The blank experiments reported by Fleischmann et al. [2] for open systems yield agreement of input and output power to within 0.003 W or better. The accuracy and precision of closed systems used by McKubre et al. [45] is stated as 0.010 W or 0.1%. The maximum excess power of 28% reported for this closed calorimetric system [45] is in good agreement with the maximum value of 27% excess power for our open system. A recent study by Storms [46] using a palladium sheet cathode in a closed isoperibolic calorimeter reports 20% excess power.

Finally, the 1 ppm detection limit for helium measurements in the effluent gases reported by Lewis et al. [42] as well as by Albagli et al. [19] is far too insensitive to detect the ^{4}He fusion product. Assuming an excess power of 1 W/cm^3 (the Pd volume was 0.31 cm^3) for deuterium fusion (eqn. (2)) would yield only 0.043 ppm of ^{4}He in the effluent gas for Lewis's study at 64 mA/cm^2 [42]. Even less helium in

the gas phase would be expected for the smaller palladium electrode ($V = 0.071$ cm^3) used in Albagli's study at 69 mA/cm^2 [19]. More sensitive analytical techniques, such as those reported here, are required for the detection of ^{4}He in the effluent gases from D$_2$O electrolysis cells.

CONCLUSIONS

Our electrochemical experiments unambiguously show a direct correlation between the time of generation of excess enthalpy and power and the production of ^{4}He, established in the absence of outside contamination. This correlation in the palladium/D$_2$O system provides strong evidence that nuclear processes are occurring in these electrolytic experiments and that helium is produced at or near the surface of the palladium rather than deeper in the bulk metal. The major gaseous fusion product in D$_2$O + LiOD is ^{4}He rather than ^{3}He. No experimental evidence for helium products, excess enthalpy or radiation is found in H$_2$O + LiOH control experiments. In summary, nuclear events with ^{4}He as a major product occur during the electrolysis of the Pd/D$_2$O + LiOD system.

ACKNOWLEDGEMENTS

REFERENCES

1 M. Fleischmann, S. Pons and M. Hawkins, J. Electroanal. Chem., 261 (1989) 301; 263 (1989) 187.
2 M. Fleischmann, S. Pons, M.W. Anderson, L.J. Li and M. Hawkins, J. Electroanal. Chem., 287 (1990) 293.
3 D.E. Stilwell, K.H. Park and M.H. Miles, J. Fusion Energy, 9 (1990) 333.
4 E.F. Mallove, Fire from Ice, Wiley, New York, 1991.
5 F. Close, Too Hot to Handle, Princeton University Press, Princeton, NJ, 1991.
6 C. Walling and J. Simons, J. Phys. Chem., 93 (1989) 4693.
7 J. Schwinger, Z. Naturforsch., 45a (1990) 756.
8 J. Schwinger, Z. Phys. D, 15 (1990) 221.
9 G. Preparata, Proc. 1st Ann. Conf. on Cold Fusion, Salt Lake City, UT, 1990, National Gold Fusion Institute, Salt Lake City, UT, p. 91.
10 T.A. Chubb and S.R. Chubb, Fusion Technol., 20 (1991) 93.

11 M.H. Miles, K.H. Park and D.E. Stilwell, J. Electroanal. Chem., 296 (1990) 241.
12 B.F. Bush, J.J. Lagowski, M.H. Miles and G.S. Ostrom, J. Electroanal. Chem., 304 (1991) 271.
13 N. Oyama, T. Ohsaka, O. Hatozaki, Y. Kurasawa, N. Yamamoto, S. Kasahara, N. Ohta, Y. Imai, Y. Oyama, T. Nakamura, T. Shibata, M. Imamura, Y. Uwamino and S. Shibata, Bull. Chem. Soc. Jpn., 63 (1990) 2659.
14 V.J. Cunnane, R.A. Scannell and D.J. Schiffrin, J. Electroanal. Chem., 269 (1989) 163.
15 J. Divisek, L. Fürst and J. Balej, J. Electroanal. Chem., 278 (1990) 99.
16 T.R. Jow, E. Plichta, C. Walker, S. Slane and S. Gilman, J. Electrochem. Soc., 137 (1990) 2473.
17 B.M. Oliver, J.G. Bradley and H. Farrar IV, Geochim. Cosmochim. Acta, 48 (1984) 1759.
18 M.H. Miles and R.E. Miles, J. Electroanal. Chem., 295 (1990) 409.
19 D. Albagli, R. Ballinger, V. Cammarata, X. Chen, R.M. Crooks, C. Fione, M.P.J. Gandreau, I. Hwang, C.K. Li, P. Linsay, S.C. Luckhardt, R.R. Parker, R.D. Petrasso, M.O. Schloh, K. W. Wenzel and M.S. Wrighton, J. Fusion Energy, 9 (1990) 133.
20 D.A. Corrigan and E.W. Schneider, J. Electroanal. Chem., 28 (1990) 305.
21 M. Srinivasan, Curr. Sci., 60 (1991) 417.
22 E. Storms, Fusion Technol., 20 (1991) 433.
23 K. Yun, J. Ju, B. Cho, W. Cho and S. Park, J. Electroanal. Chem., 306 (1991) 279.
24 E. Storms and C. Talcott, Fusion Technol., 17 (1990) 680.
25 G. Mengoli, M. Fabrizio, C. Manduchi, G. Zannoni, L. Riccardi, F. Veronesi and A. Buffa, J. Electroanal. Chem., 304 (1991) 279.
26 J. O'M. Bockris, New Sci., 129 (1752) (1991) 50.
27 J.R. Morrey, M.W. Caffee, H. Farrar IV, N.J. Hoffman, G.B. Hudson, R.H. Jones, M.D. Kunz, J. Lupton, B.M. Oliver, B.V. Ruiz, J.J. Wacker and A. Van Veen, Fusion Technol., 18 (1990) 659.
28 R.D. Petrasso, Nature (London), 350 (1991) 661.
29 S. Dushman, Scientific Foundations of Vacuum Technique (2nd edn.), Wiley, New York, 1962, pp. 491–500.
30 L. Holland, The Properties of Glass Surfaces, Chapman and Hall, London, 1964, p. 263.
31 S. Glasstone, K.J. Laidler and H. Eyring, The Theory of Rate Processes, McGraw-Hill, New York, 1941, pp. 537–544.
32 F. Paneth, Nature (London), 119 (1927) 706.
33 F. Paneth and K. Peters, Z. Phys. Chem. B, 1 (1928) 17.
34 B.Y. Liaw, P. Tao, P. Turner and B.E. Liebert, J. Electroanal. Chem., 319 (1991) 161.
35 B.Y. Liaw, P. Tao and B.E. Liebert in T. Bressani, E. Del Giudice and G. Preparata (Eds.), The Science of Cold Fusion, Conf. Proc., Vol. 33, Italian Physical Society, Bologna, 1991, p. 55.
36 S. Szpak, P.A. Mosier-Boss and J.J. Smith, J. Electroanal. Chem., 302 (1991) 255.
37 D. Lewis and K. Sköld, J. Electroanal. Chem., 294 (1990) 275.
38 L.C. Thomas, Heat Transfer, Prentice Hall, Englewood Cliffs, NJ, 1992, pp. 16–18.
39 F.T. Wagner, T.E. Moylan, M.E. Hayden, U. Narger and J.L. Booth, J. Electroanal. Chem., 295 (1990) 393.
40 J. Balej and J. Divisek, J. Electroanal. Chem., 278 (1990) 85.
41 P.A. Rock, W.H. Fink, D.A. McQuarrie, D.H. Volman and Y.F. Hung, J. Electroanal. Chem., 293 (1990) 261.
42 N.S. Lewis, C.A. Barnes, M.J. Heben, A. Kumar, S.R. Lunt, G.E. McManis, G.M. Miskelly, R.M. Penner, M.J. Sailor, P.G. Santangelo, G.A. Shreve, B.J. Tufts, M.G. Youngquist, R.W. Kavanagh, S.E. Kellogg, R.B. Vogelaar, T.R. Wang, R. Kondrat and R. New, Nature (London), 340 (1989) 525.
43 G.M. Miskelly, M.J. Heben, A. Kumar, R.M. Penner, M.J. Sailor and N.S. Lewis, Science, 246 (1989) 793.
44 D.E. Williams, D.J.S. Findlay, D.H. Craston, M.R. Sené, M. Bailey, S. Croft, B.W. Hooton, C.P. Jones, A.R.J. Kucernak, J.A. Mason and R.J. Taylor, Nature (London), 342 (1989) 375.
45 M.C.H. McKubre, R. Rocha-Filho, S.I. Smedley, F.L. Tanzella, S. Crouch-Baker, T.O. Passell and J. Santucci in T. Bressani, E. Del Giudice and G. Preparata (Eds.), The Science of Cold Fusion, Conf. Proc. Vol. 33, Italian Physical Society, Bologna, 1991, p. 419.
46 E. Storms, Fusion Technol., March (1993).